Inorganic Chemistry

Article

pubs.acs.org/IC

New Supramolecular Structural Motif Coupling a Ruthenium(II) Polyazine Light Absorber to a Rhodium(I) Center

Rongwei Zhou, Baburam Sedai, Gerald F. Manbeck, and Karen J. Brewer*

Department of Chemistry, Virginia Tech, Blacksburg, Virginia 24060-0212, United States

Supporting Information

ABSTRACT: Two new complexes, $[(bpy)_2Ru(dpp)Rh^{I}(COD)](PF_6)_3$ and $[(Me_2bpy)_2Ru(dpp)Rh^{I}(COD)](PF_6)_2(BF_4)$ (bpy = 2,2′-bipyridine, Me_2bpy = 4,4′-dimethyl-2,2′-bipyridine, dpp = 2,3-bis(2-pyridyl)pyrazine, and COD = 1,5-cyclooctadiene), representing a new Ru(II),Rh(I) structural motif, have been prepared and characterized by mass spectrometry, ^{1}H NMR spectroscopy, electrochemistry, electronic absorption spectroscopy, and emission spectroscopy. These two complexes represent a new type of supramolecular complex with a $[(TL)_2Ru(dpp)]^{2+}$ (TL = terminal ligand) light absorber (LA) coupled to a Rh(I) center and are models for Ru(II),Rh(I) intermediates in the photochemical reduction of water using dpp-bridged Ru(II),Rh(III) photocatalysts. Electrochemical study reveals overlapping reversible $Ru^{II/III}$ and irreversible $Rh^{I/II/III}$ oxidations and a quasi-reversible $dpp^{0/-}$ reduction, demonstrating that the lowest unoccupied molecular orbital (LUMO) is dpp(π^*) based. The COD ligand is sterically bulky, displaying steric repulsions between hydrogen atoms on the alkene of COD and dpp about the square planar Rh(I) center. An interesting reactivity occurs in coordinating solvents such as CH_3CN, where Rh(I) substitution leads to an equilibrium between the Ru(II),Rh(I) bimetallic and $[(TL)_2Ru(dpp)]^{2+}$ and $[Rh^{I}(COD)(solvent)_2]^{+}$ monometallic species. The electronic absorption spectra of both complexes feature transitions at ca. 500 nm attributed to a Ru(dπ) → dpp(π^*) metal-to-ligand charge transfer (MLCT) transition that is slightly red-shifted from the Ru synthon upon Rh(I) complexation. The methylation of TL on the Ru impacts the electrochemical and optical properties in a minor but predictable manner. The photophysical studies, by comparison with the model complex $[\{Ru(bpy)_2\}_2(dpp)](PF_6)_4$ and related Rh(III) complex $[(bpy)_2Ru(dpp)Rh^{III}Cl_2(phen)](PF_6)_3$, reveal the expected absence of a Ru(dπ) → Rh(dσ^*) ^{3}MMCT state (metal-to-metal charge transfer) in the title complexes, which is present in Rh(III) systems. The absence of this ^{3}MMCT state in Ru(II),Rh(I) complexes results in a longer lifetime and higher emission quantum yield for the Ru(dπ) → dpp(π^*) ^{3}MLCT state than $[(bpy)_2Ru(dpp)Rh^{III}Cl_2(phen)](PF_6)_3$. Both complexes display photocatalytic hydrogen production activity in the presence of water and a sacrificial electron donor, with the $[(bpy)_2Ru(dpp)Rh^{I}(COD)](PF_6)_3$ possessing a higher catalytic activity than the methyl analogue. Both display low activities, hypothesized to occur due to steric crowding about the Rh(I) site.

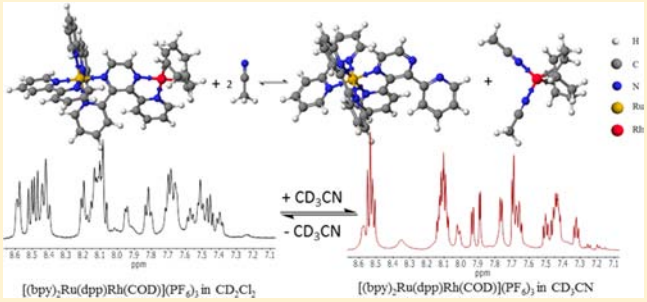

INTRODUCTION

Molecules that can act as light absorbers (LA) have been of long-term interest as light provides a means to create highly reactive electronic excited states.[1] Absorption of light generates an electronic excited state that can be highly reactive, being both a reducing and oxidizing agent. Excited state quenching processes include energy transfer or electron transfer, which with appropriate designing can utilize this excited electron or energy at the molecular level to convert light energy to electrical or chemical energy.[2,3]

One promising application of light-absorbing molecules, especially when incorporated into molecular machines, is solar water splitting to convert solar energy into hydrogen fuel. Solar water splitting is an attractive approach to address world energy demands when faced with the challenge of finite fossil fuel supplies and environmental pollution from the combustion of fossil fuels.[4−9] Hydrogen has been considered as a potential alternative energy source due to its high energy density and the product of combustion being water.[10−13] The production of hydrogen from water can be thermodynamically driven by the energy of the sun via a multielectron pathway or single-electron pathway, with the former pathway (1.23 eV) offering a much lower energy requirement than the latter (∼5 eV).[14] The low energy requirement via the multielectron pathway allows utilization of visible light to promote water splitting. Lehn et al. demonstrated in 1977 that a multicomponent system with $[Ru(bpy)_3]^{2+}$ (bpy = 2,2′-bipyridine) as LA, $[Rh(bpy)_3]^{3+}$ as electron relay, Pt colloid as a catalyst, and triethanolamine as an electron donor is capable of H_2 generation from water using visible light.[15] This encouraging result has generated vast interest among researchers to develop efficient solar water splitting systems by coupling LAs and reactive metals in complex and supramolecular assemblies.

Received: March 19, 2013
Published: November 18, 2013

   dx.doi.org/10.1021/ic4006828 | Inorg. Chem. 2013, 52, 13314−13324

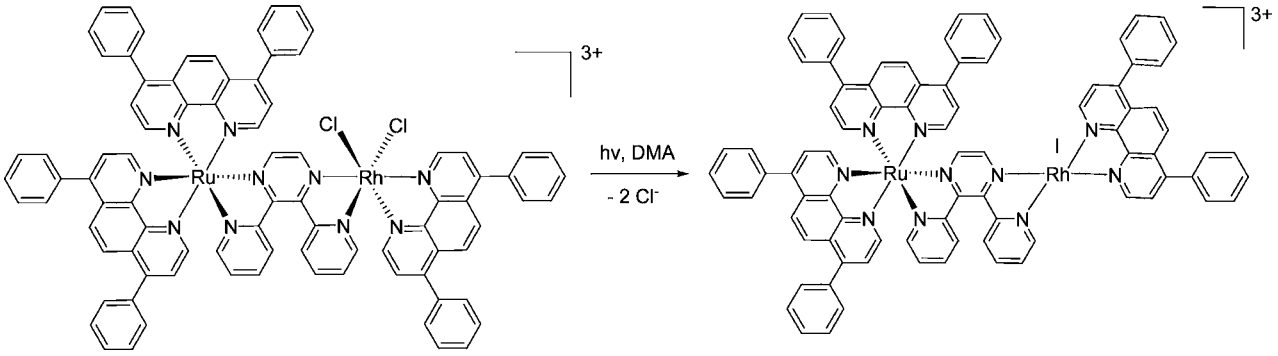

Figure 1. Photoinitiated electron collection at the Rh center of the supramolecular complex $[(Ph_2phen)_2Ru(dpp)Rh^{III}Cl_2(Ph_2phen)](PF_6)_3$ forming the two-electron-reduced $[(Ph_2phen)_2Ru(dpp)Rh^{I}(Ph_2phen)](PF_6)_3$ through halide loss upon visible light irradiation in the presence of an electron donor.[29,30]

Covalent coupling of subunits while maintaining the individual properties of each subunit can generate supramolecular complexes with new functions.[1] Supramolecules containing LA(s) can perform photoinitiated electron transfer to generate charge separation. Collecting multiple electrons is a challenging process due to the Coulombic barrier to bringing two electrons together. The first example of a functional supramolecular complex for photoinitiated electron collection is $[\{(bpy)_2Ru(dpb)\}_2IrCl_2]^{3+}$ (bpy = 2,2′-bipyridyl, dpb = 2,3-bis(2-pyridyl)benzoquinoxaline).[16] This molecule reversibly collects two electrons on π^* orbitals of the two dpb bridging ligands. MacDonnell and Campagna reported several interesting Ru bimetallic complexes that can photochemically collect up to four electrons at the π^* orbitals of the bridging ligands.[17−19] Photoinitiated electron accumulation at the metal center was later accomplished in $[(NC)_5M^{II}(CN)\text{-}Pt^{IV}(NH_3)_4(NC)M^{II}(CN)_5]^{4+}$ (M = Fe, Ru, or Os); however, reduction to Pt(II) leads to decomposition.[20] A proton-coupled two-electron transfer was observed in the Ru monometallic $[(bpy)_2Ru(pbn)]^{2+}$ to form $[(bpy)_2Ru(pbnHH)]^{2+}$ (pbn = 2-(2-pyridyl)benzo[*b*]-1,5-naphthyridine).[21,22] These early photoinitiated electron collectors were not photocatalytically active toward hydrogen production from water as they collected electrons on nonreactive sites.

The first LA-incorporated supramolecular complex that acts as a photoinitiated electron collector and a photocatalyst for water reduction was $[\{(bpy)_2Ru(dpp)\}_2Rh^{III}Cl_2](PF_6)_5$ (dpp = 2,3-bis(2-pyridyl)pyrazine).[23−27] The architecture incorporates two Ru(II) LAs, and when excited with visible light in the presence of *N*,*N*-dimethylaniline (DMA) as an electron donor, this supramolecule can collect two electrons on the Rh(III) center, resulting in the reduction of Rh^{III} to Rh^{I} accompanied by loss of chlorides and generation of two reducing equivalents, which can be utilized to reduce H_2O to H_2.[23−26] Further modification of this trimetallic architecture improved photocatalytic activity and provided insight into the mechanism of reduction.[28,29] Recent studies were extended to eliminate one LA to give a Ru(II),Rh(III) bimetallic complex, which initially was an inactive photocatalyst.[29] Careful tuning of the electronics and sterics led to the first dpp-bridged Ru(II),Rh(III) bimetallic photocatalyst $[(Ph_2phen)_2Ru(dpp)\text{-}Rh^{III}Cl_2(Ph_2phen)]^{3+}$ (Ph_2phen = 4,7-diphenyl-1,10-phenanthroline).[30] Spectrophotochemical and spectroelectrochemical analyses, in conjunction with mass spectrometry data, support the formation of a Ru(II),Rh(I) intermediate species (Figure 1) in a same manner as $[\{(bpy)_2Ru(dpp)\}_2Rh^{I}](PF_6)_5$.[29,30] While it is likely that a Ru(II),Rh(I) species plays a critical role in the photocatalytic cycle during hydrogen production, isolation and direct characterization of mixed metal species of this oxidation state are rare due to the high reactivity of Rh(I) species in this motif.

Several Rh^{I} complexes have been reported as intermediates in water reduction catalysis. The generation of a Rh^{I} species was found in Lehn's multicomponent system. Protonation resulted in the formation of a Rh hydride species that, as well as $[Rh^{I}(bpy)_2]^{+}$, can dimerize and deactivate the catalytic system.[3,31−33] Fujita, Creutz, and co-workers showed the reaction of $[Rh^{I}(bpy)_2]^{+}$ and H_2 can produce *cis*-$[Rh^{III}(bpy)_2(H)_2]^{+}$, which can reductively eliminate H_2 under photolysis.[34,35] The Wilkinson's catalyst analogue $[Rh^{I}Cl\text{-}(dpm)_3]^{3-}$ (dpm = diphenylphosphinobenzene-*m*-sulfonate) can photochemically reduce water to give H_2 in the presence of $[Ru(bpy)_3]^{2+}$ and ascorbic acid.[36] Dinuclear Rh^{I}−Rh^{I} bridged by 1,3-diisocyanopropane can catalytically produce hydrogen under visible light irradiation in acidic conditions.[37,38] Nocera has established a dinuclear mixed-valence rhodium system capable of reducing hydrohalic acids to hydrogen in the presence of a halogen trap.[39] An Os(II),Rh(I) bimetallic complex, $[\{(tpyPh(m\text{-}Ph_2P))_2Os\}Rh^{I}Cl(CO)]^{2+}$, bearing a $[Os(tpy)_2]^{2+}$ (tpy = 2,2′:6′,2″-terpyridyl) moiety as LA, was proposed to be an intermediate in the photocatalytic water reduction in a multicomponent system involving the $[Os\text{-}(tpy)_2]^{2+}$ LA and $RhCl_3$.[40] These studies highlight the importance of Rh^{I} in metal hydride chemistry and catalytic steps needed to reduce water to hydrogen. A preliminary result of a Ru(II),Rh(I) system has been reported by Inagaki.[41,42]

To probe the factors impacting the functioning and deactivation of the Ru(II),Rh(I) complex in dpp-bridged Ru(II),Rh(III),Ru(II) or Ru(II),Rh(III) systems, independent syntheses of Ru(II) bridged by dpp to Rh(I) systems are needed. Herein we report the synthesis, characterization, and photochemical study of two new dpp-bridged Ru(II),Rh(I) complexes, $[(bpy)_2Ru(dpp)Rh^{I}(COD)](PF_6)_3$ and $[(Me_2bpy)_2Ru(dpp)Rh^{I}(COD)](PF_6)_2(BF_4)$, describing properties and reactivity.

EXPERIMENTAL SECTION

Materials. All reactions were performed under argon using either glovebox or Schlenk line techniques. All solvents and chemicals were used as purchased unless otherwise noted. Extra dry grade dichloromethane (99.8%) and acetone (99.8%) were purchased from Acros Organics. The complex $[Rh^{I}(COD)_2](BF_4)$ was purchased from Strem Chemicals. All deuterated solvents were used as received.

dx.doi.org/10.1021/ic4006828 | *Inorg. Chem.* 2013, 52, 13314−13324

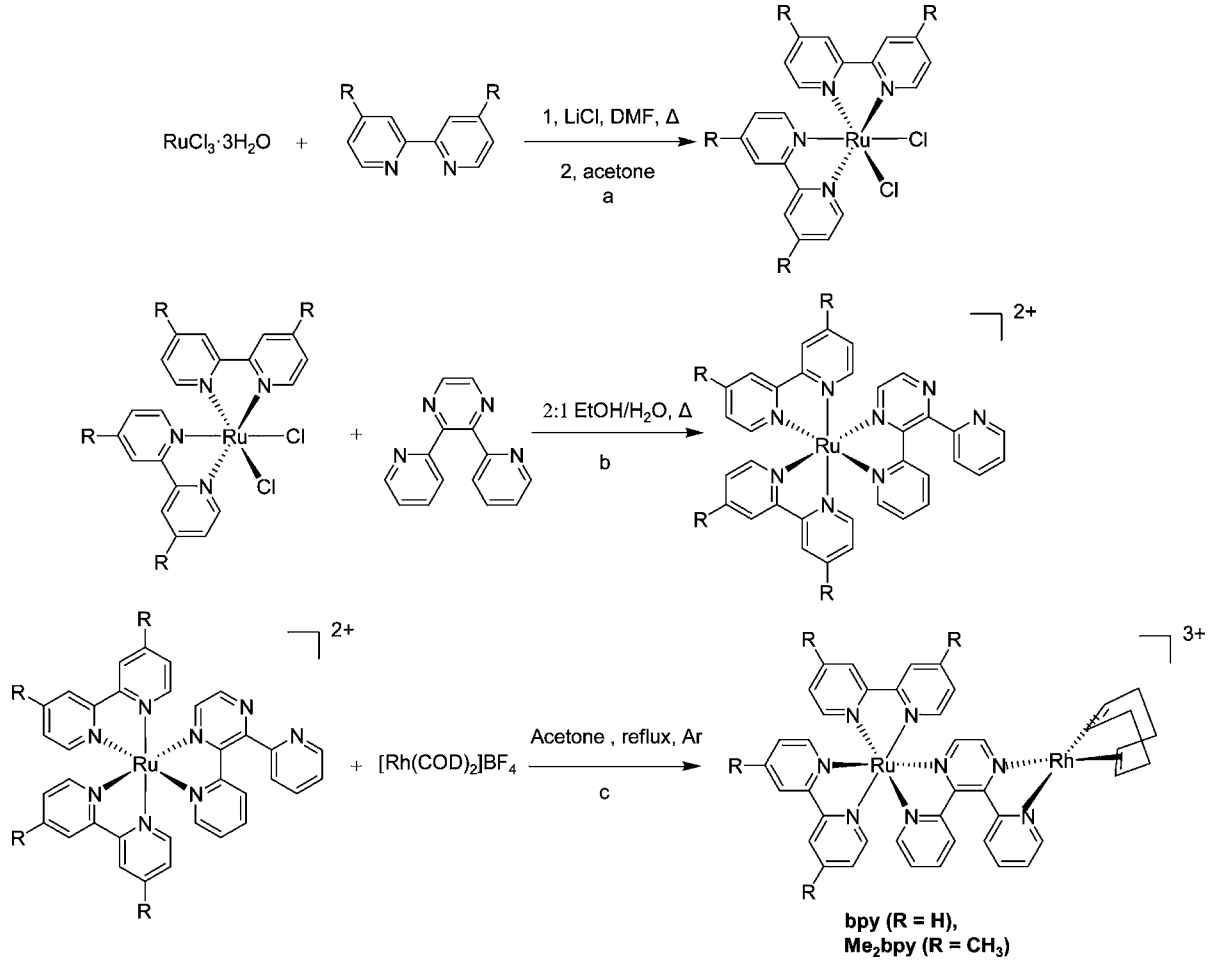

Figure 2. Synthetic scheme of $[(bpy)_2Ru(dpp)Rh^I(COD)](PF_6)_3$ and $[(Me_2bpy)_2Ru(dpp)Rh^I(COD)](PF_6)_2(BF_4)$. [a]Adapted from ref 44. [b]Adapted from ref 43. [c]Adapted from ref 41.

Samples for $^1H-^1H$ NOESY and $^1H-^1H$ COSY analysis were deoxygenated with three freeze–pump–thaw cycles. ^1H NMR, $^1H-^1H$ NOESY, and $^1H-^1H$ COSY spectra were recorded on a JEOL 500 MHz NMR spectrometer at 298 K. The complexes $[(bpy)_2Ru(dpp)](PF_6)_2$, $[(Me_2bpy)_2Ru(dpp)](PF_6)_2$, $[(bpy)_2Ru(dpp)Rh^{III}Cl_2(phen)](PF_6)_3$, and $[\{Ru(bpy)_2\}_2(dpp)](PF_6)_4$ were prepared as previously described.[43−45] Mass spectrometry was recorded on an Agilent Technologies 6220 Accurate Mass TOF LC-MS with a dual ESI source in acetone or acetonitrile.

Synthesis of $[(bpy)_2Ru(dpp)Rh^I(COD)](PF_6)_3$. The starting material $[Rh^I(COD)_2](BF_4)$ (0.10 g, 0.25 mmol) and $[(bpy)_2Ru(dpp)](PF_6)_2$ (0.19 g, 0.21 mmol) were dissolved in acetone (5.0 mL) in a Schlenk flask under argon at room temperature. The mixture was stirred for 5 h, after which the solvent was removed under vacuum. Diethyl ether (ca. 5 mL) was added to wash the residue. The solid was dissolved in acetone and added to 30 mL of saturated KPF_6 aqueous solution to induce precipitation of the PF_6^- salt. The precipitate was collected by vacuum filtration and washed with water (ca. 10 mL), ethanol (ca. 5 mL × 2), and diethyl ether (ca. 10 mL × 3). The precipitate was then dried under vacuum to afford 0.21 g (0.16 mmol) of $[(bpy)_2Ru(dpp)Rh^I(COD)](PF_6)_3$ as a pink-purple solid in 75% yield. ^1H NMR (500 MHz, CD_2Cl_2, RT): δ 2.00 (br, 2H, COD), 2.35 (br, 2H, COD), 2.47 (br, 2H, COD), 2.81 (br, 2H, COD), 4.67 (br, 4H, COD), 7.40–8.61 (26 H, Ar–H). ESI-MS (acetone): $[M - PF_6]^+$, m/z calcd 1149.06, found 1149.0615.

Synthesis of $[(Me_2bpy)_2Ru(dpp)Rh^I(COD)](PF_6)_2(BF_4)$. The above method has been used to prepare $[(Me_2bpy)_2Ru(dpp)Rh^I(COD)](PF_6)_2(BF_4)$ using $[(Me_2bpy)_2Ru(dpp)](PF_6)_2$ (0.21 g, 0.21 mmol) without metathesis to the PF_6^- salt with an isolated yield of 80% (0.22 g, 0.17 mmol). ^1H NMR (500 MHz, CD_2Cl_2, RT): δ 1.95 (br, 2H, COD), 2.35 (br, 2H, COD), 2.47 (br, 2H, COD), 2.56 (s, 6H, CH_3), 2.59 (s, 3H, CH_3), 2.61 (s, 3H, CH_3), 2.81 (br, 2H, COD), 4.67 (br, 4H, COD), 7.40–8.61 (22H, Ar–H). ESI-MS (acetone): $[M - BF_4]^+$, m/z calcd 1205.12, found 1205.1113

Electrochemistry. Cyclic voltammograms were obtained using a Bioanalytical Systems (BAS) Epsilon electrochemical analyzer with a three-electrode, single-compartment cell. The supporting electrolyte was a 0.1 M solution of tetrabutylammonium hexafluorophosphate (Bu_4NPF_6) in deoxygenated and dry dichloromethane. A platinum disk and platinum wire were used for the working electrode and the auxiliary electrode, respectively. An Ag wire was used as a pseudoreference electrode and was calibrated against the ferrocene/ferrocenium couple ($FeCp_2^{+/0}$ = 0.46 V vs Ag/AgCl 3 M NaCl) as an internal standard.[46] The cyclic voltammograms were obtained at a scan rate of 100 mV/s. Solutions were purged with Ar prior to analysis and blanked with Ar during data collection.

Electronic Absorption Spectroscopy. The electronic absorption spectra were obtained using a Hewlett-Packard 8452A diode array spectrometer at room temperature with 2 nm resolution and an integration time of 0.5 s. The samples were measured in dry and deoxygenated dichloromethane using a 1 cm quartz cuvette (Starna Cells Inc.; Atascadero, CA, USA). The molar extinction coefficient measurements were performed in triplicate.

Emission Spectroscopy. The room-temperature emission spectra were collected in deoxygenated dry dichloromethane solution using a 1 cm path length quartz cuvette. The spectra were recorded in a Quanta model QM-200-45E fluorometer from Photon Technologies International, Inc. The source of excitation was a water-cooled 150 W xenon arc lamp, with the corresponding emission collected at a 90° angle using a thermoelectrically cooled Hamamatsu 1527 photo-

dx.doi.org/10.1021/ic4006828 | Inorg. Chem. 2013, 52, 13314−13324

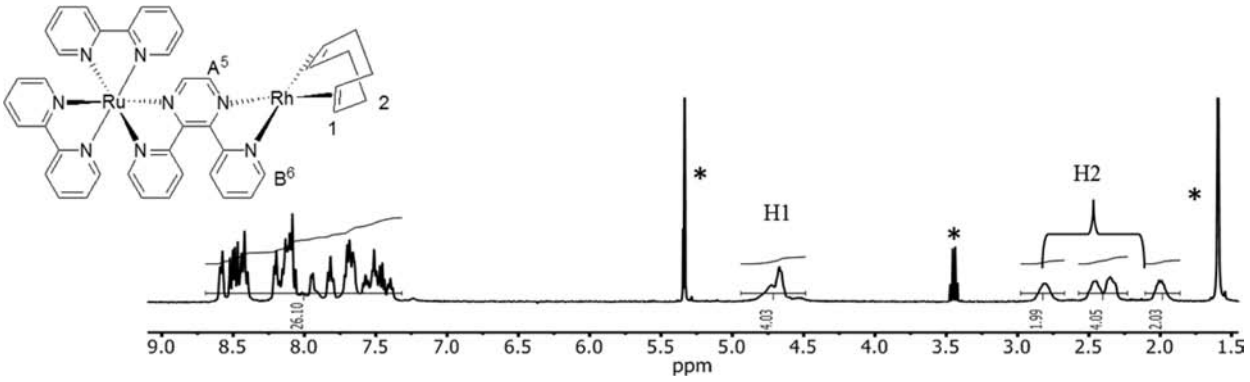

Figure 3. ^{1}H NMR spectrum of $[(bpy)_2Ru(dpp)Rh^I(COD)](PF_6)_3$ in CD_2Cl_2. Solvent resonance peaks are marked by *.

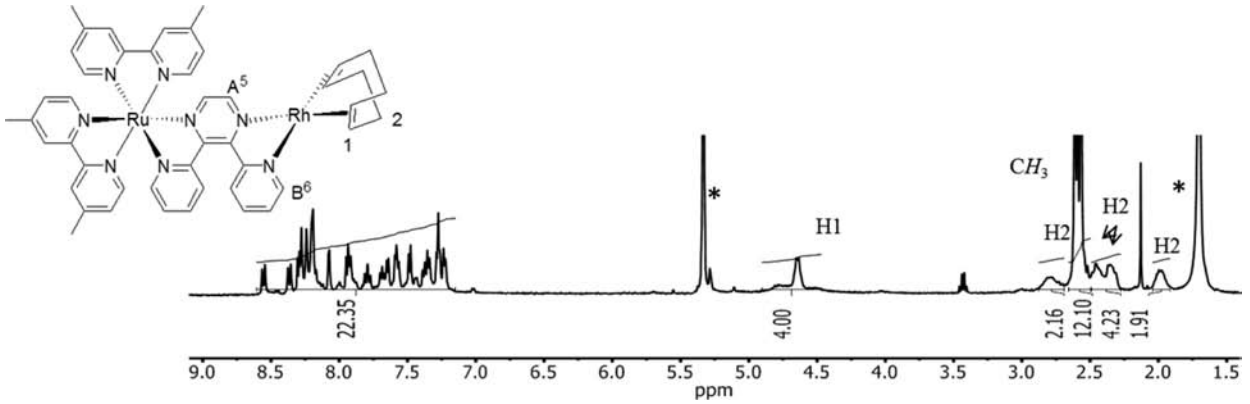

Figure 4. ^{1}H NMR spectrum of $[(Me_2bpy)_2Ru(dpp)Rh^I(COD)](PF_6)_2(BF_4)$in CD_2Cl_2. Solvent resonance peaks are marked by *.

multiplier tube operating in photon counting mode with 0.25 nm resolution. The quantum yield was measured in CH_2Cl_2 with a similar absorbance at 460 nm for monometallic complexes and 520 nm for each bimetallic complex and was referenced to $[Os(bpy)_3](PF_6)_2$ in CH_3CN ($\Phi = 4.6 \times 10^{-3}$) using eq 1, where I_s is the integrated emission area of the sample, I_r is the integrated emission area of the reference, n_s is the refractive index of the sample solvent, n_r is the refractive index of the reference solvent, A_r is the absorbance of the reference, and A_s is the absorbance of the sample. Φ_r is the quantum yield of the reference, and Φ_s is the quantum yield of the sample.[47] The 77 K emission spectra were measured in a rigid glass matrix prepared from toluene/CH_2Cl_2 (1.1:1 v/v) submerged in a liquid N_2 filled finger dewar. The monometallic synthons were excited at 460 nm, and bimetallics were excited at 520 nm. The emission spectra were corrected for PMT response.

$$\Phi_s = \frac{A_r \times I_s \times n_s^2}{A_s \times I_r \times n_r^2} \times \Phi_r \quad (1)$$

Excited State Lifetime Measurements and Data Analysis. The excited state lifetimes were recorded from a Photon Technologies International, Inc. PL-2300 nitrogen laser equipped with a PL-201 tunable dye laser as excitation source. The dye used was Coumarin 500, and the excitation monochromator was set to 460 nm for monometallic complexes and 520 nm for bimetallic complexes. Sample emission signals were collected at 90° from the excitation source through a monochromator set at λ_{max}^{em} for each sample and detected using a Hamamatsu R928 photomultiplier tube operating in direct analog mode. The signal was recorded using a LeCroy 9361 oscilloscope, averaging the results of 300 pulses, and transferred to a computer for data analysis. A single-exponential function, $Y = A + Be^{-x/\tau}$ (τ is lifetime in seconds) was fit to the data profile. Room-temperature measurements were made in an argon-saturated dichloromethane solution.

Equations 2 and 3 were used to calculate k_r (rate constant for radiative decay) and k_{nr} (rate constant for nonradiative decay) of Ru monometallic synthons, the title Ru(II),Rh(I) complexes, and the $[\{(bpy)_2Ru\}_2(dpp)](BF_6)_4$ model complex.[47,48] In order to calculate k_{et} (rate constant for intramolecular electron transfer) for $[(bpy)_2Ru(dpp)Rh^{III}Cl_2(phen)](PF_6)_3$, the k_n and k_{nr} from the $[\{(bpy)_2Ru\}_2(dpp)](BF_6)_4$ model complex were used in eqs 4 and 5.[6]

$$\Phi^{em} = \frac{k_r}{k_r + k_{nr}} \quad (2)$$

$$\tau = \frac{1}{k_r + k_{nr}} \quad (3)$$

$$\Phi^{em} = \frac{k_r}{k_r + k_{nr} + k_{et}} \quad (4)$$

$$\tau = \frac{1}{k_r + k_{nr} + k_{et}} \quad (5)$$

Photochemistry. Photocatalytic hydrogen production experiments were performed using previously reported conditions substituting acetone as the solvent in place of acetonitrile or DMF.[23] A solution containing acetone, the bimetallic complex, and water was deoxygenated using argon gas in the photolysis reaction cells capped with airtight septa. DMA was deoxygenated separately and added to the reaction cells just prior to photolysis (final solution = 4.46 mL; 65 μM bimetallic complex, 1.5 M DMA, 0.62 M H_2O, headspace = 15.5 mL). The samples were photolyzed from the bottom of the cells using a 470 nm LED light source array constructed in our laboratory (light flux = $2.36 \pm 0.05 \times 10^{19}$ photons/min). The amount of H_2 produced was monitored in real time using an HY-OPTIMA 700 in-line process solid state H_2 sensor from H2Scan connected to the photolysis reaction cell. The total amount of hydrogen produced in the photolysis

dx.doi.org/10.1021/ic4006828 | Inorg. Chem. 2013, 52, 13314−13324

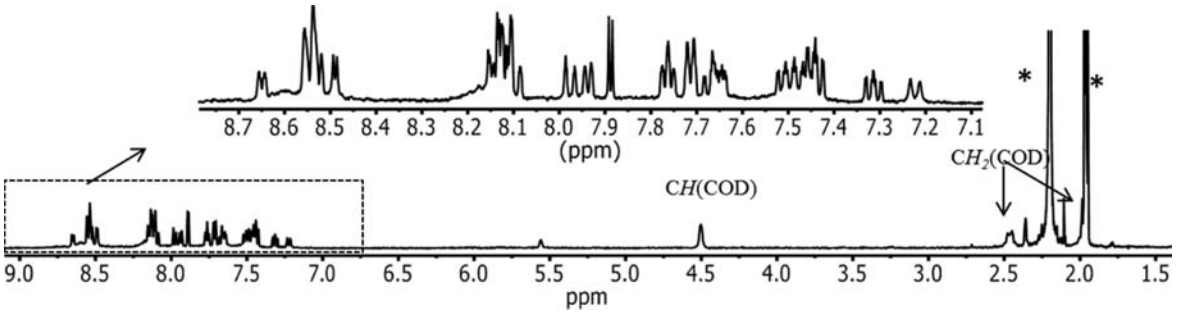

Figure 5. ^{1}H NMR spectrum of $[(bpy)_2Ru(dpp)Rh^I(COD)](PF_6)_3$ in CD_3CN. Solvent resonance peaks are marked by *.

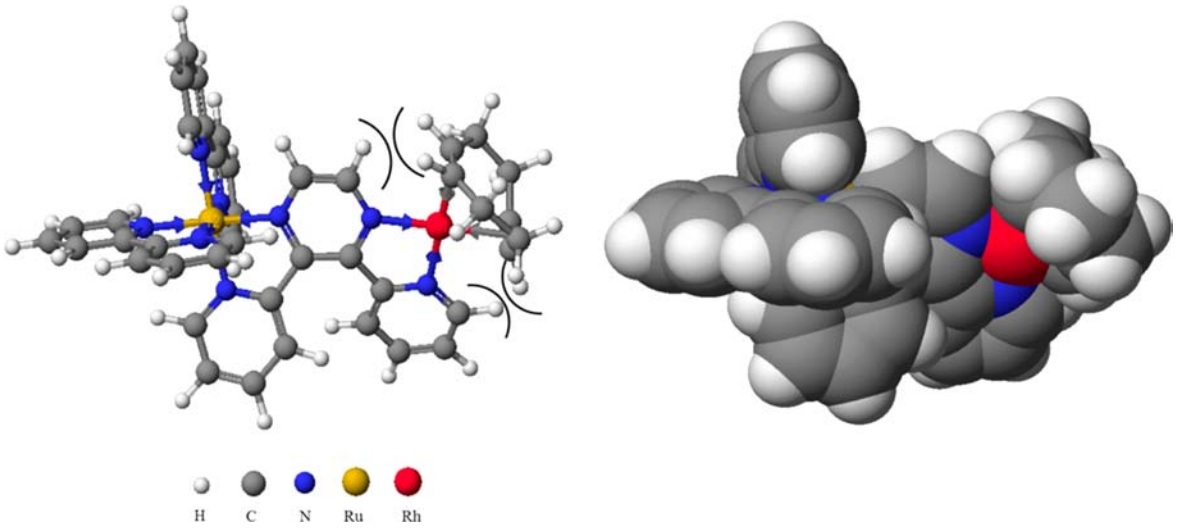

Figure 6. Graphic and space-filling representation of $[(bpy)_2Ru(dpp)Rh^I(COD)]^{3+}$ showing the repulsion between protons on the dpp ligand and alkene protons of COD.

experiment was determined using a calibration curve. The reported value for hydrogen production is the average of three experiments.

RESULTS AND DISCUSSION

Synthesis. The two new Ru(II),Rh(I) bimetallic complexes have been prepared in a good yield using a building block approach (Figure 2). The terminal ligand (TL) was reacted with $RuCl_3 \cdot 3H_2O$ in DMF with excess LiCl to give $[(TL)_2RuCl_2]$. The reaction of $[(TL)_2RuCl_2]$ with a slight excess of dpp afforded $[(TL)_2Ru(dpp)](PF_6)_2$. The Ru(II),Rh(I) bimetallic compounds were prepared in a high yield by treating monometallic synthons, $[(TL)_2Ru(dpp)](PF_6)_2$ with 1.2 equiv of $[Rh^I(COD)_2](BF_4)$ under argon in acetone.[41] The title compounds were soluble in acetone and CH_2Cl_2 and were stable under ambient light and temperature conditions.

Characterization. The $[(bpy)_2Ru(dpp)Rh^I(COD)](PF_6)_3$, $[(Me_2bpy)_2Ru(dpp)Rh^I(COD)](PF_6)_2(BF_4)$, and the Ru monometallic synthons were characterized by ^{1}H NMR spectroscopy and electrospray ionization mass spectrometry (ESI-MS). The assignments of ^{1}H NMR spectra of two monometallic synthons in CD_2Cl_2 (Supporting Information, Figures S1 and S2) are based on 2D ^{1}H−^{1}H COSY and the spectrum of $[(bpy)_2Ru(dpp)](PF_6)_2$ in CD_3CN and D_2O + D_2SO_4.[49,50] The chemical shifts of the dpp A^5 proton and four H^3 protons on the bpy ring are slightly different in CD_2Cl_2 and CD_3CN. It should be noticed that the bipyridine H^6 protons exhibit different chemical shifts due to intrinsic asymmetry of these complexes and ring current effects. The ^{1}H NMR spectra of bimetallic complexes are provided in Figure 3 and Figure 4. In both bimetallic complexes, four nonequivalent proton resonances of the allylic positions of COD are observed from 2 to 3 ppm with the integration ratio of 1:1:1:1 due to the expected inequivalence of these protons. The vinyl proton resonance of COD is observed around 4.7 ppm and is shifted upfield compared to free COD (5.5 ppm), supporting the coordination to Rh(I). The protons on COD in $[(bpy)_2Ru(dpp)Rh^I(COD)](PF_6)_3$, and $[(Me_2bpy)_2Ru(dpp)Rh^I(COD)](PF_6)_2(BF_4)$ appear as broad signals, indicating possible fluctional behavior of the COD ring due to steric repulsion by the close dpp A^5 and B^6 atoms.[51,52] The aromatic resonances in the bimetallic ^{1}H NMR spectra correctly integrate to 26 protons for $[(bpy)_2Ru(dpp)Rh^I(COD)](PF_6)_3$ and 22 protons for the Me_2bpy analogue, assuming the area of the vinyl proton of COD corresponds to 4 protons. The assignment of each aromatic proton is complicated by the overlap of the protons' resonance, but two protons in the dpp ligand can be assigned using the 2D ^{1}H−^{1}H NOESY technique (Figures S3, S4). Two spatial coupling signals with vinyl COD are observed and assigned to protons A^5 and B^6 on the dpp ring, reaffirming the coordination of dpp with the Rh(I)COD unit and demonstrating that the complex remains intact in solution. The chemical shifts of these two protons are similar in both complexes and shift upfield with respect to the monometallic synthons due to the coordination of the electron-rich Rh^I center.

dx.doi.org/10.1021/ic4006828 | Inorg. Chem. 2013, 52, 13314−13324

The new Ru(II),Rh(I) binuclear compounds exhibit different ^{1}H NMR spectra in CD_3CN from CD_2Cl_2, resulting from the steric repulsion between the vinyl COD protons and A[5] and B[6] on dpp and ligating properties of acetonitrile. Both complexes display similar behavior in CD_3CN, and the detailed study of $[(bpy)_2Ru(dpp)Rh^I(COD)](PF_6)_3$ is described as an example (Figure 5). Compared to the ^{1}H NMR spectrum in CD_2Cl_2, the vinyl COD protons slightly shift upfield (4.5 ppm). Only two resonances of the allylic COD protons at 2.4 and 1.9 ppm are observed, in contrast to the four signals in CD_2Cl_2, suggesting a change in symmetry around the Rh(I) center in CD_3CN. The aromatic resonances are better resolved than in CD_2Cl_2. Noticeably, the aromatic protons on both bpy and dpp are similar to those of free $[(bpy)_2Ru(dpp)]^{2+}$ in CD_3CN (Figure S5). The ^{1}H NMR spectrum change in CD_3CN can be explained by the formation of $[(bpy)_2Ru(dpp)]^{2+}$ and $[Rh^I(COD)(CD_3CN)_2]^+$ in equilibrium with the bimetallic $[(bpy)_2Ru(dpp)Rh^I(COD)]^{3+}$.[41] If the CD_3CN solution of the title bimetallic $[(bpy)_2Ru(dpp)Rh^I(COD)]^{3+}$ in equilibrium with the monometallic Ru(II) and Rh(I) species is evaporated to dryness and dissolved in CD_2Cl_2, the original spectrum of $[(bpy)_2Ru(dpp)Rh^I(COD)]^{3+}$ is obtained. The presence of $[(bpy)_2Ru(dpp)](PF_6)^+$ (m/z = 793.09), $[Rh^I(COD)(CH_3CN)_2]^+$ (m/z = 293.05), $[(dpp)Rh^I(COD)]^+$ (m/z = 445.09), and $[\{(bpy)_2Ru(dpp)Rh^I(COD)\}(PF_6)_2]^+$ (m/z = 1149.06) in the ESI mass spectrum of $[(bpy)_2Ru(dpp)Rh^I(COD)](PF_6)_3$ in CH_3CN reaffirms this interesting reactivity of Ru(II),Rh(I) in ligating solvent, whereby an equilibrium mixture of these species is obtained (Figure S7). This interesting new reactivity is attributed to the strong ligating effect of acetonitrile and steric repulsion of the alkene hydrogens in COD with the A[5] and B[6] hydrogens on dpp, as shown in the Figure 6. Since equilibrium mixtures of intact bimetallics $[(bpy)_2Ru(dpp)]^{2+}$ and $[Rh^I(COD)(CD_3CN)_2]^+$ are present in CD_3CN, all further studies were carried out in CH_2Cl_2 or acetone.

Electrochemistry. The cyclic voltammograms of $[(bpy)_2Ru(dpp)Rh^I(COD)](PF_6)_3$ and $[(Me_2bpy)_2Ru(dpp)Rh^I(COD)](PF_6)_2(BF_4)$ were recorded in CH_2Cl_2, and the electrochemical assignments are listed in Table 1. For comparison, voltammograms of $[(bpy)_2Ru(dpp)](PF_6)_2$ and $[(Me_2bpy)_2Ru(dpp)](PF_6)_2$ were measured under the same conditions. Cyclic voltammograms of monometallic synthons are similar in CH_2Cl_2 and CH_3CN with Ru-based oxidations and ligand-based reductions.[53] The reversible $Ru^{III/II}$ redox couple of $[(bpy)_2Ru(dpp)](PF_6)_2$ appears at 1.47 V vs Ag/AgCl (Figure 7). Upon changing the TL from bpy to Me_2bpy, the reversible $Ru^{III/II}$ couple shifts cathodically to 1.39 V vs Ag/AgCl, consistent with the electron-donating nature of the methyl substituents. Reductively, monometallic complexes display two reversible couples around −1.0 and −1.5 V vs Ag/AgCl, which are assigned as $dpp^{0/-}$ followed by $bpy^{0/-}$ or $Me_2bpy^{0/-}$ reductions, respectively. This assignment indicates the LUMO in each complex is dpp(π^*) based and the HOMO is Ru(dπ) based.

Cyclic voltammograms of the bimetallic complexes exhibit quasi-reversible oxidations and two quasi-reversible reduction couples. In comparison to $[(TL)_2Ru(dpp)](PF_6)_2$ as shown in Table 1, coordination to the Rh(I) fragment causes a slight positive shift of ca. 100 mV in the $Ru^{III/II}$ couple consistent with stabilization of the Ru(dπ) orbital energy due to increased back-bonding to the bridging dpp ligand and the increased positive charge of the complexes. The quasi-reversible oxidation

Table 1. Electrochemical Data in CH_2Cl_2 and Assignments for the Title Ru(II),Rh(I) Complexes and Monometallic Synthons

complex[a]	$E_{1/2}$ (V vs Ag/AgCl)[b]	assignment
$[(bpy)_2Ru(dpp)]^{2+}$	1.47 (58 mV)	$Ru^{III/II}$
	−1.03 (78 mV)	$dpp^{0/-}$
	−1.53 (76 mV)	$bpy^{0/-}$
$[(bpy)Ru(dpp)Rh^I(COD)]^{3+}$	1.57 (130 mV)	$Ru^{III/II}$, $Rh^{I/II/III}$
	−0.53 (50 mV)	$dpp^{0/-}$
	−1.21 (49 mV)	$dpp^{-/2-}$
$[(Me_2bpy)_2Ru(dpp)]^{2+}$	1.39 (51 mV)	$Ru^{III/II}$
	−1.01 (42 mV)	$dpp^{0/-}$
	−1.59 (50 mV)	$Me_2bpy^{0/-}$
$[(Me_2bpy)_2Ru(dpp)Rh^I(COD)]^{3+}$	1.52 (150 mV)	$Ru^{III/II}$, $Rh^{I/II/III}$
	−0.47 (55 mV)	$dpp^{0/-}$
	−1.15 (60 mV)	$dpp^{-/2-}$

[a] bpy = 2,2′-bipyridine, Me_2bpy = 4,4′-dimethyl-2,2′-bipyridine, dpp = 2,3-bis(2-pyridyl)pyrazine, and COD = 1,5-cyclooctadiene. [b] Recorded in 0.1 M Bu_4NPF_6 in CH_2Cl_2 with potential reported in V vs Ag/AgCl, using a Ag wire pseudoreference electrode and ferrocene internal standard ($FeCp_2^{+/0}$ = 0.46 V vs Ag/AgCl). The numbers in parenthese are ΔE_p.

occurs at $E_{1/2}$ = 1.57 V, ΔE_p = 130 mV vs Ag/AgCl, with $i_p^a > i_p^c$ for $[(bpy)_2Ru(dpp)Rh^I(COD)](PF_6)_3$. The Me_2bpy analogue displays a quasi-reversible oxidation at $E_{1/2}$ = 1.52 V, ΔE_p = 150 mV vs Ag/AgCl, and $i_p^a > i_p^c$. The quasi-reversible oxidation waves include an overlapping reversible $Ru^{II/III}$ oxidation couple and irreversible $Rh^{I/II/III}$ oxidations. Because of this overlap and the irreversible nature of the rhodium oxidation, an increased anodic current is observed relative to the cathodic current. Reductively, two quasi-reversible couples in the bimetallic complexes are assigned as sequential single-electron reduction of the bridging ligand, $dpp^{0/-}$ and $dpp^{-/2-}$. The first reduction occurs at −0.53 V vs Ag/AgCl in $[(bpy)_2Ru(dpp)Rh^I(COD)](PF_6)_3$ and at −0.47 V vs Ag/AgCl in $[(Me_2bpy)_2Ru(dpp)Rh^I(COD)](PF_6)_2(BF_4)$. These reductions are shifted cathodically relative to the $dpp^{0/-}$ couple of the Ru(II) synthons, indicating a small stabilization of dpp (π^*) orbitals upon coordination of the Rh^I center. An increase of the cathodic current in the first reduction couple as shown by the bottom dotted line in Figure 7 is observed in both bimetallic complexes when scanning positively first to pass through the irreversible $Rh^{I/II/III}$ couple, illustrative of $Rh^{III/II/I}$ reduction occurring in the region as a result of Rh^{III} generated via the oxidative scan. This also validates the assignment of $Rh^{I/II/III}$ in the oxidation couple. The electrochemistry is consistent with a Ru(dπ)-based HOMO and a dpp(π^*)-based LUMO.

The $[(bpy)_2Ru(dpp)Rh^I(COD)](PF_6)_3$ complex exhibits different electrochemical properties from previously reported Ru(II),Rh(III) complex $[(bpy)_2Ru(dpp)Rh^{III}Cl_2(phen)](PF_6)_3$, which bears the same light-absorber unit. The cyclic voltammogram of $[(bpy)_2Ru(dpp)Rh^{III}Cl_2(phen)](PF_6)_3$ displays a reversible $Ru^{II/III}$ oxidation couple at 1.61 V vs Ag/AgCl, which is more positive than $[(bpy)_2Ru(dpp)Rh^I(COD)](PF_6)_3$.[45] Whereas the reductive cyclic voltammogram of $[(bpy)_2Ru(dpp)Rh^I(COD)](PF_6)_3$ exhibits ligand-based reductions only, the cyclic voltammogram of $[(bpy)_2Ru(dpp)Rh^{III}Cl_2(phen)](PF_6)_3$ displays $Rh^{III/II}$ and $Rh^{II/I}$ reductions prior to the $dpp^{0/-}$ couple. The electrochemical assignments indicate a Ru(dπ)-based HOMO and a Rh(dσ^*)-based LUMO

dx.doi.org/10.1021/ic4006828 | Inorg. Chem. 2013, 52, 13314−13324

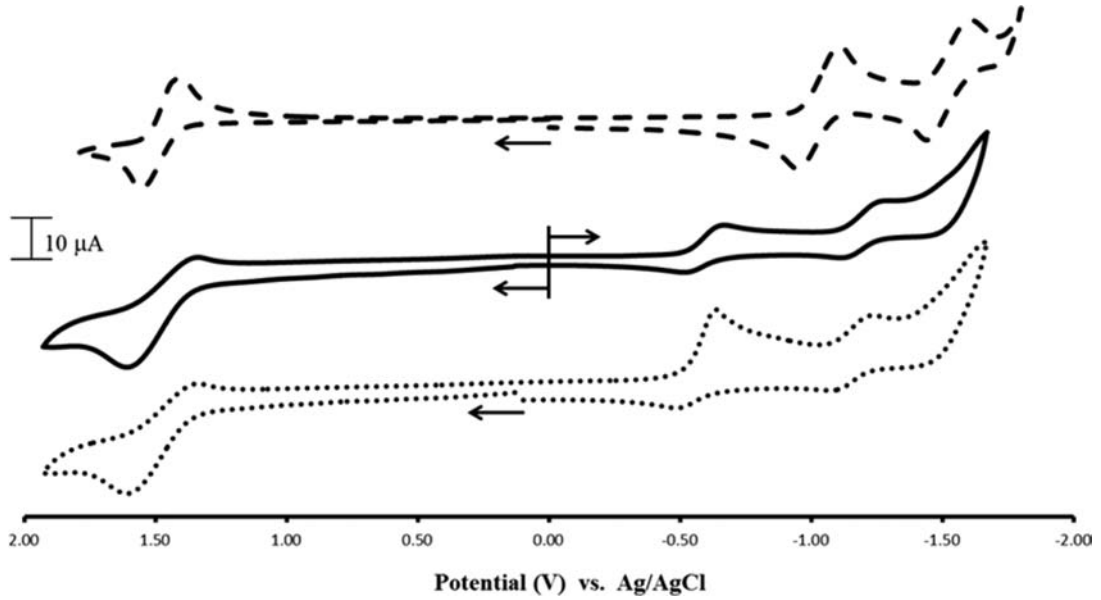

Figure 7. Cyclic voltammograms of $[(bpy)_2Ru(dpp)](PF_6)_2$ (top, dashed line) and $[(bpy)_2Ru(dpp)Rh^{I}(COD)](PF_6)_3$ (middle, solid line, and bottom dotted line) in 0.1 M $^{t}Bu_4NPF_6$ in CH_2Cl_2 solution using a platinum disk working electrode, platinum wire auxiliary electrode, and silver wire as reference electrode ($FeCp_2^{+/0}$ = 0.46 V vs Ag/AgCl). Scan direction is indicated by an arrow (bpy = 2,2′-bipyridine, dpp = 2,3-bis(2-pyridyl)pyrazine, and COD = 1,5-cyclooctadiene).

in $[(bpy)_2Ru(dpp)Rh^{III}Cl_2(phen)](PF_6)_3$. In the new title Ru(II),Rh(I) complexes the HOMO is still Ru(dπ)-based, but the LUMO is dpp(π^*)-based. The change of the oxidation state of Rh provides orbital inversion of these bimetallic complexes, which should impact the photophysical properties (*vide infra*).

Electronic Absorption Spectroscopy. The electronic absorption spectra of the bimetallic complexes and monometallic synthons are shown in Figure 8 and are summarized in Table 2. In both monometallic and bimetallic complexes, the UV or near-UV region is dominated by intraligand (IL) $\pi \rightarrow \pi^*$ transitions, with dpp-based $\pi \rightarrow \pi^*$ transitions underlying the intense TL $\pi \rightarrow \pi^*$ transitions in the monometallic and appearing as a low-energy shoulder at ca. 340 nm in the title bimetallics, leading to a reduction in the intensity of the peak ca. 286 nm upon Rh(I) complexation. The absorption bands in the visible region are assigned as Ru(dπ) → bpy(π^*) CT transitions at higher energy and Ru(dπ) → dpp(π^*) CT at lower energy in both bimetallics and monometallics.[48] The Ru(dπ) → dpp(π^*) CT transition red shifts to ca. 500 nm due to the stabilized dpp(π^*) orbital upon coordination of the Rh(I)(COD) unit. In comparison with $[(bpy)_2Ru(dpp)Rh^{I}(COD)](PF_6)_3$, the lowest energy Ru(d$\pi$) → dpp($\pi^*$) CT absorption in $[(Me_2bpy)_2Ru(dpp)Rh^{I}(COD)](PF_6)_2(BF_4)$ is slightly red-shifted, consistent with the decrease of the energy gap between the Ru(dπ)-based HOMO and dpp(π^*)-based LUMO observed electrochemically.

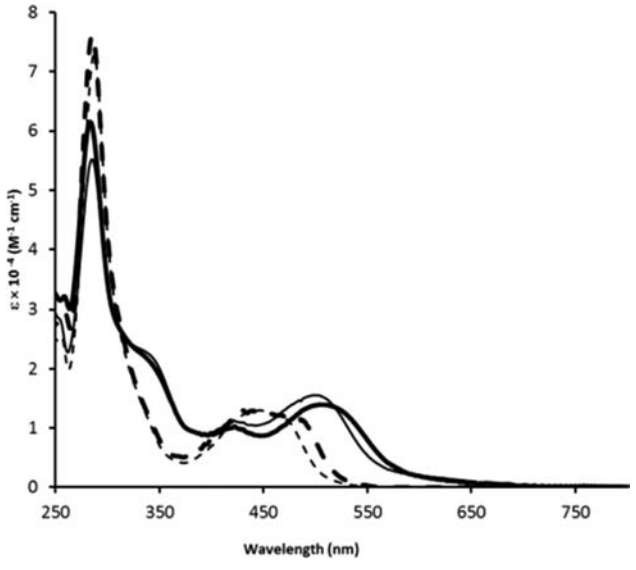

Figure 8. Electronic absorption spectra for the $[(bpy)_2Ru(dpp)Rh^{I}(COD)](PF_6)_3$ (—), $[(bpy)_2Ru(dpp)](PF_6)_2$ (- -), $[(Me_2bpy)_2Ru(dpp)Rh^{I}(COD)](PF_6)_2(BF_4)$ (——), and $[(Me_2bpy)_2Ru(dpp)](PF_6)_2$ (– –) measured in deoxygenated dry CH_2Cl_2 at room temperature (bpy = 2,2′-bipyridine, Me_2bpy = 4,4′-dimethyl-2,2′-bipyridine, dpp = 2,3-bis(2-pyridyl)pyrazine, and COD = 1,5-cyclooctadiene).

Emission Spectroscopy. Ru(II) polyazine complexes are known to undergo photoexcitation by visible light to a ^{1}MLCT excited state that populates an emissive ^{3}MLCT state via intersystem crossing typically with unit efficiency, providing a probe into excited state dynamics.[6,54] Emission spectroscopy and excited state lifetimes of the Ru monometallic synthons, the title Ru(II),Rh(I) complexes, and the homonuclear bimetallic model complex $[\{Ru(bpy)_2\}_2(dpp)](BF_6)_4$ have been measured at room temperature in deaerated CH_2Cl_2 and at 77 K, and the results are provided in Table 3 and Figure 9. For comparison, $[(bpy)_2Ru(dpp)Rh^{III}Cl_2(phen)](PF_6)_3$ was chosen to represent Ru(II),Rh(III) bimetallic systems, and the photophysical data are also included in Table 3.

Upon excitation at 460 nm, the monometallic complexes display emissions with λ_{max}^{em} = 665 nm for $[(bpy)_2Ru(dpp)](PF_6)_2$ and λ_{max}^{em} = 680 nm for $[(Me_2bpy)_2Ru(dpp)](PF_6)_2$, attributed to the Ru(d$\pi$) → dpp($\pi^*$) ^{3}MLCT excited state. The red shift of the emission band in $[(Me_2bpy)_2Ru(dpp)](PF_6)_2$

dx.doi.org/10.1021/ic4006828 | *Inorg. Chem.* 2013, 52, 13314–13324

Table 2. Electronic Absorption Spectra and Assignments for Title Ru(II),Rh(I) Complexes and Monometallic Synthons

complex[a]	λ_{max}^{abs} (nm)	$\varepsilon \times 10^{-4}$ (M^{-1} cm^{-1})	assignment
$[(bpy)_2Ru(dpp)]^{2+}$	287	7.28	bpy,dpp $\pi \rightarrow \pi^*$
	435	1.29	Ru(dπ) $\rightarrow$ bpy(π^*) CT
	462	1.20	Ru(dπ) $\rightarrow$ dpp(π^*) CT
$[(bpy)_2Ru(dpp)Rh^{I}(COD)]^{3+}$	285	5.52	bpy $\pi \rightarrow \pi^*$
	330	2.34	dpp $\pi \rightarrow \pi^*$
	425	1.17	Ru(dπ) $\rightarrow$ bpy(π^*) CT
	501	1.55	Ru(dπ) $\rightarrow$ dpp(π^*) CT
$[(Me_2bpy)_2Ru(dpp)]^{2+}$	286	7.60	Me_2bpy, dpp $\pi \rightarrow \pi^*$
	435	1.27	Ru(dπ) $\rightarrow$ Me_2bpy(π^*) CT
	485	1.18	Ru(dπ) $\rightarrow$ dpp(π^*) CT
$[(Me_2bpy)_2Ru(dpp)Rh^{I}(COD)]^{3+}$	284	6.14	Me_2bpy $\pi \rightarrow \pi^*$
	334	2.24	dpp $\pi \rightarrow \pi^*$
	421	1.01	Ru(dπ) $\rightarrow$ Me_2bpy(π^*) CT
	508	1.39	Ru(dπ) $\rightarrow$ dpp(π^*) CT

[a]Recorded in CH_2Cl_2 at room temperature (bpy =2,2′-bipyridine, Me_2bpy = 4,4′-dimethyl-2,2′-bipyridine, dpp = 2,3-bis(2-pyridyl)pyrazine, and COD = 1,5-cyclooctadiene).

Table 3. Summary of Photophysical Data in Deoxygenated CH_2Cl_2 at Room Temperature and at 77 K

	RT[b]						77 K[c]	
complex[a]	λ_{max}^{em} (nm)	Φ^{em} ($\times 10^3$)[d]	τ (ns)[e]	$k_r \times 10^{-4}$ (s^{-1})[f]	$k_{nr} \times 10^{-6}$ (s^{-1})[f]	$k_{et} \times 10^{-7}$ (s^{-1})[f]	λ_{max}^{em} (nm)	τ (μs)[e]
$[(bpy)_2Ru(dpp)]^{2+}$	665 (667)[g]	16 (15)[g]	480 (450)[g]	11	2.0		620, 665	6.0
$[(bpy)_2Ru(dpp)Rh^{I}(COD)]^{3+}$	705	1.6	130	1.3	7.7		690	2.4
$[(Me_2bpy)_2Ru(dpp)]^{2+}$	680 (685)[g]	14	390 (390)[g]	7.7	2.5		630, 660	6.0
$[(Me_2bpy)_2Ru(dpp)Rh^{I}(COD)]^{3+}$	720	1.3	100	1.4	9.9		700	2.3
$[\{(bpy)_2Ru\}_2(dpp)]^{4+}$	745 (770)[g]	3.5	160 (154)[g]	2.3	6.2		700	2.8
$[(bpy)_2Ru(dpp)RhCl_2(phen)]^{3+}$	760	1.0	55	2.3	6.2	1.6	710	2.0

[a]bpy = 2,2′-bipyridine, Me_2bpy = 4,4′-dimethyl-2,2′-bipyridine, dpp = 2,3-bis(2-pyridyl)pyrazine, phen = 1,10-phenanthroline, and COD = 1,5-cyclooctadiene. [b]Recorded in deaerated CH_2Cl_2 at room temperature. [c]Measured in toluene/CH_2Cl_2 (1.1:1 v/v) rigid matrix at 77 K. [d]Measured as a relative quantum yield using $[Os(bpy)_3]^{2+}$ in CH_3CN and reported value of $\Phi \pm 3\%$. [e]Reported value of $\tau \pm 10\%$. [f]k_r = rate constant for radiative decay, k_{nr} = rate constant for nonradiative decay, k_{et} = rate constant for electron transfer. [g]Values from ref 48 in CH_2Cl_2.

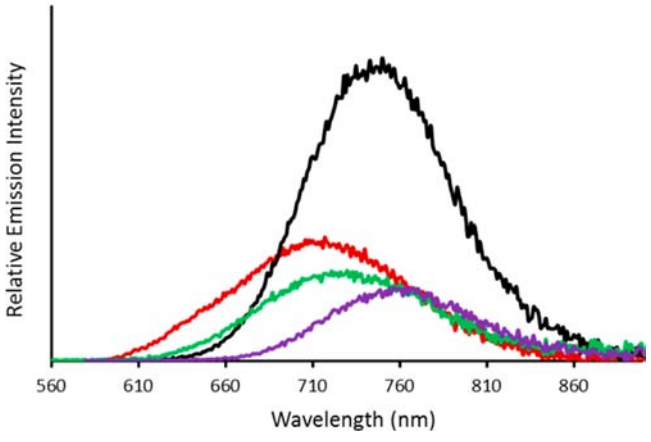

Figure 9. Emission spectra for $[\{(bpy)_2Ru\}_2(dpp)](PF_6)_4$ (black), $[(bpy)_2Ru(dpp)Rh^{I}(COD)](PF_6)_3$ (red), $[(Me_2bpy)_2Ru(dpp)Rh^{I}(COD)](PF_6)_2(BF_4)$ (green), and $[(bpy)_2Ru(dpp)Rh^{III}Cl_2(phen)](PF_6)_3$ (purple) measured in deoxygenated dry CH_2Cl_2 at room temperature absorbance matched at 520 nm, the wavelength of excitation, to allow direct comparison of emission intensity (bpy = 2,2′-bipyridine, Me_2bpy = 4,4′-dimethyl-2,2′-bipyridine, dpp = 2,3-bis(2-pyridyl)pyrazine, phen = 1,10-phenanthroline, and COD = 1,5-cyclooctadiene).

relative to $[(bpy)_2Ru(dpp)](PF_6)_2$ is in agreement with the electrochemistry and electronic absorption spectroscopy. The methylation in the TL results in a weaker emission and a shorter lifetime for the ^{3}MLCT state than the bpy analogue, $\Phi^{em} = 1.6 \times 10^{-2}$ (τ = 480 ns) for $[(bpy)_2Ru(dpp)](PF_6)_2$ and $\Phi^{em} = 1.4 \times 10^{-2}$ (τ = 390 ns) for $[(Me_2bpy)_2Ru(dpp)](PF_6)_2$, which can be predicted from the energy gap law and the expected enhanced nonradiative decay (k_{nr}) of 2.5×10^6 s^{-1} in the Me_2bpy complex vs 2.0×10^6 s^{-1} in the bpy complex.[48,55] At 77 K, both monometallic synthon emissions show structure emissions at ca. 620 nm and shoulders at ca. 660 nm, similar to literature reported data (Figure S8).[48] Emission lifetimes at 77 K in toluene/CH_2Cl_2 (1.1:1, v/v) glass are ca. 6.0 μs for both monometallics, as shown in Table 3. The lifetimes at 77 K glass are slightly higher than literature reported values in 4:1 ethanol/methanol glass (4.06 μs for $[(Me_2bpy)_2Ru(dpp)](PF_6)_2$ and 5.36 μs for $[(bpy)_2Ru(dpp)](PF_6)_2$) due to the difference of the rigid matrix.

The coordination of Ru monometallic synthons to the Rh(I) center to form the title Ru(II),Rh(I) bimetallics results in a red shift of emission band relative to the corresponding monometallic synthon. The emission centers at λ_{max}^{em} = 705 nm for $[(bpy)_2Ru(dpp)Rh^{I}(COD)](PF_6)_3$ and λ_{max}^{em} = 720 nm for $[(Me_2bpy)_2Ru(dpp)Rh^{I}(COD)](PF_6)_2(BF_4)$. The red shift is consistent with the lower lying dpp (π^*) orbital after coordination to the Rh(I) center observed in the electrochemistry and spectroscopy. Compared to the monometallic synthons, the emission intensity and lifetime of Ru(dπ) $\rightarrow$ dpp(π^*) ^{3}MLCT in the bimetallic complexes are significantly reduced, with an emission quantum yield of 1.6×10^{-3} for

dx.doi.org/10.1021/ic4006828 | Inorg. Chem. 2013, 52, 13314−13324

$[(bpy)_2Ru(dpp)Rh^{I}(COD)](PF_6)_3$ (τ = 130 ns) and 1.3×10^{-3} for $[(Me_2bpy)_2Ru(dpp)Rh^{I}(COD)](PF_6)_2(BF_4)$ (τ = 100 ns), respectively. The reduced excited state lifetimes and quantum yields of emission upon coupling can be attributed to the lower lying ^{3}MLCT excited states relative to the monometallic synthons. The enhanced k_{nr} in $[(Me_2bpy)_2Ru(dpp)Rh^{I}(COD)](PF_6)_2(BF_4)$ ($k_{nr} = 9.9 \times 10^6$ s^{-1}) vs $[(bpy)_2Ru(dpp)Rh^{I}(COD)](PF_6)_3$ ($k_{nr} = 7.7 \times 10^6$ s^{-1}) can account for the lower quantum yield of $[(Me_2bpy)_2Ru(dpp)Rh^{I}(COD)](PF_6)_2(BF_4)$. At low temperature, the λ_{max}^{em} of the title bimetallics is blue-shifted with an enhancement of excited state lifetime to ca. 2.3 μs (Figure S8).

The title Ru(II),Rh(I) bimetallics, $[(bpy)_2Ru(dpp)Rh^{I}(COD)](PF_6)_3$, exhibit a higher quantum yield, longer excited state lifetime, and higher energy ^{3}MLCT excited state than the analogous Ru(II),Rh(III) bimetallics, $[(bpy)_2Ru(dpp)Rh^{III}Cl_2(phen)](PF_6)_3$ ($\Phi^{em} = 1.0 \times 10^{-3}$, τ = 55 ns, λ_{max}^{em} = 760 nm). In comparison to the $[\{(bpy)_2Ru\}_2(dpp)](PF_6)_4$ model complex ($\Phi^{em} = 3.5 \times 10^{-3}$, τ = 160 ns), the new Ru(II),Rh(I) complexes are slightly weaker emitters with shortened excited state lifetimes. At 77 K, $[(bpy)_2Ru(dpp)Rh^{I}(COD)](PF_6)_3$ and $[(bpy)_2Ru(dpp)Rh^{III}Cl_2(phen)](PF_6)_3$ exhibited excited state lifetimes of 2.4 and 2.0 μs, respectively. These lifetimes are comparable to the Ru(II),Ru(II) model complex (τ = 2.8 μs). For the Ru(II),Rh(III) complexes such as $[(bpy)_2Ru(dpp)Rh^{III}Cl_2(phen)](PF_6)_3$, formation of a low-lying ^{3}MMCT state via intramolecular electron transfer (k_{et}) has been proposed as a pathway for deactivation of the emissive ^{3}MLCT state.[45,56] Applying the k_n and k_{nr} in the Ru(II),Ru(II) model complex in eq 4, the k_{et} in $[(bpy)_2Ru(dpp)Rh^{III}Cl_2(phen)](PF_6)_3$ was obtained as 1.6×10^7 s^{-1} . At 77 K, this intramolecular electron transfer to form the nonemissive ^{3}MMCT is impeded. As a result, the lifetime of the ^{3}MLCT in $[(bpy)_2Ru(dpp)Rh^{III}Cl_2(phen)](PF_6)_3$ (τ = 2.0 μs) is comparable to model Ru(II),Ru(II) systems.[45] The title Ru(II),Rh(I) systems have more intense emission and longer lived Ru(dπ) → dpp(π*) ^{3}MLCT states than the analogous Ru(II),Rh(III) systems due to the absence of low-lying Ru(dπ) → Rh(dσ*) ^{3}MMCT states as a mode of deactivation of the emissive excited states.

Photocatalysis. The proposed photocatalytically active intermediate of Ru(II),Rh(III) supramolecular photocatalysts for water reduction to produce H_2 is Ru(II),Rh(I) in nature. Photocatalytic hydrogen production experiments were performed using the newly synthesized Ru(II),Rh(I) bimetallics. It was hypothesized that the steric crowding about the Rh(I) center would lead to poor catalytic performance. Investigating the photocatalytic hydrogen production of the title Ru(II),Rh(I) bimetallics will provide insight into the role of Rh(I) in the more active Ru(II),Rh(I) intermediates produced by the photoreduction of the Ru(II),Rh(III) complexes where terminal diimine ligands are bound to the photogenerated Rh(I) site. Photocatalytic experiments with the new bimetallic complexes were conducted in acetone due to the equilibrium mixture of species in CH_3CN as observed by ^{1}H NMR. In the presence of DMA (1.5 M), water (0.62 M), and light flux ($2.36 \pm 0.05 \times 10^{19}$ photons/min), both title complexes generate hydrogen (Figure S9). After a 20 h photolysis at 470 nm, $[(bpy)_2Ru(dpp)Rh^{I}(COD)](PF_6)_3$ produced 49 ± 5 μmol of H_2, 170 ± 30 TON (TON = turnover number = mole of H_2 produced per mole of Ru(II),Rh(I) catalyst), and 0.20% overall efficiency. The $[(Me_2bpy)_2Ru(dpp)Rh^{I}(COD)](PF_6)_2(BF_4)$ complex produced consistently lower amounts of hydrogen with 17 ± 2 μmol of H_2, 60 ± 7 TON, and 0.08% overall efficiency. The complex $[(bpy)_2Ru(dpp)Rh^{III}Cl_2(phen)](PF_6)_3$ is nearly inactive under similar conditions due to Rh(I)−Rh(I) bond formation upon photoreduction to lead to deactivation of the catalyst.[57] The steric protection imparted by the COD ligand allows the title complexes to be photocatalysts. However the steric repulsion between COD and dpp about the Rh(I) center may lead to deactivation of hydrogen production from this motif over time, as considerable steric rearrangement and ligand addition and elimination are needed in the photocatalytic cycle. The change of TL from bpy to Me_2bpy results in the decrease of the catalytic activity consistent with electronic properties of the light absorber playing an important role in photocatalysis.[30,58] Addition of a large excess of Hg(l) does not impact the functioning of the photocatalytic systems with similar turnovers, suggesting that intact supramolecules and not colloidal Rh(s) is active in this system.

Table 4. Photocatalytic Hydrogen Production[a]

complex	H_2 (μmol)	TON[b]
$[(bpy)_2Ru(dpp)Rh^{I}(COD)]^{3+}$	49 ± 5	170 ± 30
$[(Me_2bpy)_2Ru(dpp)Rh^{I}(COD)]^{3+}$	17 ± 2	60 ± 7

[a]Values shown are after 20 h of the photolysis using a 470 nm LED light source (light flux = $(2.36 \pm 0.05) \times 10^{19}$ photons/min; solution volume = 4.5 mL; head space volume = 15.5 mL). [b]TON = turnover number (mole of H_2 produced per mole of catalyst).

Previous works have proposed that Ru(II),Rh(I) bimetallics are the active species for photocatalytic hydrogen production from water in $[(TL)_2Ru^{II}(dpp)Rh^{III}(Cl)_2(TL)]^{3+}$ systems.[29,30] This predicted that Ru(II),Rh(I) species may stoichiometrically reduce H_2O to H_2. However the title Ru(II),Rh(I) complexes are inactive in H_2 production without an electron donor, even in acidified water. This may be reflective of the varied sterics and electronics imparted by COD ligand or imply that further reduction is needed prior to activation. Future work is directed toward the replacement of COD with polypyridyl ligands to provide additional Ru(II),Rh(I) systems for the investigation of the photocatalytic water reduction mechanism by Ru(II),Rh(III) and Ru(II),Rh(III),Ru(II) complexes.

CONCLUSIONS

The new Ru(II),Rh(I) motif has been prepared and studied. The complexes undergo a new interesting reaction to provide a mixture of species in strong ligating solvents due to steric repulsion between the COD alkene hydrogens and the dpp hydrogens. Both complexes exhibit a quasi-reversible oxidation couple containing the reversible $Ru^{II/III}$ oxidation couple and the $Rh^{I/II/III}$ irreversible oxidation couple at similar potentials. Electrochemistry reveals the Ru(dπ)-based HOMO and dpp(π*)-based LUMO in these two new Ru(II),Rh(I) complexes. The change of TL results in a slight decrease of HOMO to LUMO energy gap, which is unveiled by electrochemical studies and spectroscopy. Both complexes possess emissive ^{3}MLCT excited states with lower emission energy, quantum yield of emission, and excited state lifetime relative to the Ru synthons, consistent with dpp(π*) acceptor stabilization upon Rh(I) addition. The absence of low-lying Ru(dπ) → Rh(dσ*) ^{3}MMCT states can account for the higher emission quantum yield and lifetime of the title Ru(II),Rh(I) systems relative to analogous Ru(II),Rh(III) systems. The

methylation of bpy leads to a slight decrease in quantum yield and lifetime of ^{3}MLCT excited states with an increase of k_{nr}. In the presence of light, DMA, and H_2O, these two Ru(II),Rh(I) complexes display photocatalytic activity to produce H_2 in contrast to the sterically accessible $[(bpy)_2Ru(dpp)$-$RhCl_2(phen)]^{3+}$, which dimerizes upon photoreduction to generate the Rh(I) state. Low efficiency for H_2 production shown in Ru(II),Rh(I) likely results from the steric repulsion in this complex that may result in impeded interaction with substrates and steric constraint of the structural rearrangements needed during the photocatalytic cycle. The different activity between two complexes differing by the TL indicates the TL can influence the catalytic activity through modulation of the ^{3}MLCT excited state energy and lifetime. This study reports detailed analysis of basic chemical, photophysical, and photochemical properties of the Ru(II),Rh(I) class of compounds, providing insight for future molecular design of additional members of this important structural motif.

■ ASSOCIATED CONTENT

Supporting Information

^{1}H NMR spectra of monometallic complexes in CD_3CN and CD_2Cl_2, ^{1}H−^{1}H NOSY spectra, ESI-MS, and hydrogen production profile. This material is available free of charge via the Internet at http://pubs.acs.org.

■ AUTHOR INFORMATION

Corresponding Author

*E-mail: Kbrewer@bt.edu.

Notes

The authors declare no competing financial interest.

■ ACKNOWLEDGMENTS

Acknowledgment is made to the U.S. Department of Energy DEFG 02-05ER15751 for their generous financial support of our research. The authors also give thanks to Dr. Shamindri M. Arachchige, Dr. Travis White, Dr. Jessica Knoll, Dr. Jing Wang, and Dr. Akiko Inagaki for their helpful suggestions during the work.

■ REFERENCES

(1) Balzani, V.; Moggi, L.; Manfrin, M. F.; Bolletta, F.; Laurence, G. S. *Coord. Chem. Rev.* **1975**, *15*, 321−433.
(2) Arachchige, S. M.; Brewer, K. J. In *Macromolecules Containing Metal and Metal-Like Elements: Supramolecular and Self-Assembled Metal-Containing Materials*; John Wiley & Sons, Inc.: New York, 2009; pp 295−368
(3) Brown, G. M.; Chan, S. F.; Creutz, C.; Schwarz, A. H.; Sutin, N. *J. Am. Chem. Soc.* **1979**, *101*, 7638−7640.
(4) Balzani, V.; Bergamini, G.; Campagna, S.; Puntoriero, F. *Top. Curr. Chem.* **2007**, *280*, 1−36.
(5) Balzani, V.; Moggi, L.; Scandola, F. In *Supramolecular Photochemistry*; Balzani, V., Ed.; Reidel: Dordrecht, 1987; Vol. *214*, pp 1−28.
(6) Kalyanasundaram, K. *Coord. Chem. Rev.* **1982**, *46*, 159−244.
(7) Armaroli, N.; Balzani, V. *Angew. Chem., Int. Ed.* **2007**, *46*, 52−66.
(8) Armaroli, N.; Balzani, V. *Chem.−Asian J.* **2011**, *6*, 768−784.
(9) Armaroli, N.; Balzani, V. *Energy Environ. Sci.* **2011**, *4*, 3193−3222.
(10) Esswein, A. J.; Veige, A. S.; Nocera, D. G. *J. Am. Chem. Soc.* **2005**, *127*, 16641−16651.
(11) Esswein, A. J.; Nocera, D. G. *Chem. Rev.* **2007**, *107*, 4022−4047.
(12) Nocera, D. G. *Inorg. Chem.* **2009**, *48*, 10001−10017.
(13) Armaroli, N.; Balzani, V. *ChemSusChem* **2011**, *4*, 21−36.
(14) Bard, A. J.; Fox, M. A. *Acc. Chem. Res.* **1995**, *28*, 141−145.
(15) Lehn, J. M.; Sauvage, J. P. *Nouv. J. Chim.* **1977**, *1*, 449−451.
(16) Molnar, S. M.; Nallas, G.; Birdgewater, J. S.; Brewer, K. J. *J. Am. Chem. Soc.* **1994**, *116*, 5206−5210.
(17) Konduri, R.; Ye, H.; MacDonnell, F. M.; Serroni, S.; Campagna, S.; Rajeshwar, K. *Agnew. Chem. Int. Ed.* **2002**, *41*, 3185−3187.
(18) Chiorboli, C.; Fracasso, S.; Scandola, F.; Campagna, S.; Serroni, S.; Konduri, R.; MacDonnell, F. M. *Chem. Commun.* **2003**, 1658−1659.
(19) Chiorboli, C.; Fracasso, S.; Ravaglia, M.; Scandola, F.; Campagna, S.; Wouters, K. L.; Konduri, R.; MacDonnell, F. M. *Inorg. Chem.* **2005**, *44*, 8368−8378.
(20) Chang, C. C.; Pfennig, B.; Bocarsly, A. B. *Coord. Chem. Rev.* **2000**, *208*, 33−45.
(21) Polyansky, D.; Cabelli, D.; Muckerman, J. T.; Fujita, E.; Koizumi, T.; Fukushima, T.; Wada, T.; Tanaka, K. *Angew. Chem., Int. Ed.* **2007**, *46*, 4169−4172.
(22) Polyansky, D.; Cabelli, D.; Muckerman, J. T.; Fukushima, T.; Tanaka, K.; Fujita, E. *Inorg. Chem.* **2008**, *47*, 3958−3968.
(23) Arachchige, S. M.; Brown, J.; Brewer, K. J. *J. Photochem. Photobiol. A: Chem.* **2008**, *197*, 13−17.
(24) Arachchige, S. M.; Brown, J.; Chang, E.; Jain, A.; Zigler, D. F.; Rangan, K.; Brewer, K. J. *Inorg. Chem.* **2009**, *48*, 1989−2000.
(25) Elvington, M.; Brewer, K. J. *Inorg. Chem.* **2006**, *45*, 5242−5244.
(26) Elvington, M.; Brown, J.; Arachchige, S. M.; Brewer, K. J. *J. Am. Chem. Soc.* **2007**, *129*, 10644−10645.
(27) Rangan, K.; Arachchige, S. M.; Brown, J. R.; Brewer, K. J. *Energy Environ. Sci.* **2009**, *2*, 410−419.
(28) White, T. A.; Higgins, S. L. H.; Arachchige, S. M.; Brewer, K. J. *Agnew. Chem. Int. Ed.* **2011**, *50*, 12209−12213.
(29) Wang, J.; White, T. A.; Arachchige, S. M.; Brewer, K. J. *Chem. Commun.* **2011**, *47*, 4451−4453.
(30) White, T. A.; Whitaker, B. N.; Brewer, K. J. *J. Am. Chem. Soc.* **2011**, *133*, 15332−15334.
(31) Kirch, M.; Lehn, J. M.; Sauvage, J. P. *Helv. Chim. Acta* **1979**, *62*, 1345−1384.
(32) Chan, S. F.; Chou, M.; Creutz, C.; Matsubara, T.; Sutin, N. *J. Am. Chem. Soc.* **1981**, *103*, 369−379.
(33) Mulazzani, Q. G.; Emmi, S.; Hoffman, M. Z.; Venturi, M. *J. Am. Chem. Soc.* **1981**, *103*, 3362−3370.
(34) Yan, S. G.; Brunschwig, B. S.; Creutz, C.; Fujita, E.; Sutin, N. *J. Am. Chem. Soc.* **1998**, *120*, 10553−10554.
(35) Fujita, E.; Brunschwig, B. S.; Creutz, C.; Muckerman, J. T.; Sutin, N.; Szalda, D.; Eldik, R. *Inorg. Chem.* **2006**, *45*, 1595−1603.
(36) Oishi, S. *J. Mol. Catal.* **1987**, *39*, 225−232.
(37) Mann, K. R.; Lewis, N. S.; Miskowski, V. M.; Erwin, D. K.; Hammond, G. S.; Gray, H. B. *J. Am. Chem. Soc.* **1977**, *99*, 5525−5526.
(38) Mann, K. R.; Bell, R. A.; Gray, H. B. *Inorg. Chem.* **1979**, *18*, 2671−2673.
(39) Heyduk, A. F.; Nocera, D. G. *Science* **2001**, *293*, 1369−1641.
(40) Miyake, Y.; Nakajima, K.; Sasaki, K.; Saito, R.; Nakanishi, H.; Nishibayashi, Y. *Organometallics* **2009**, *28*, 5240−5243.
(41) Saita, T.; Nitadori, H.; Inagaki, A.; Akita, M. *J. Organomet. Chem.* **2009**, *694*, 3125−3133.
(42) Inagaki, A.; Nakagawa, H.; Akita, M.; Inoue, T.; Sakai, M.; Fujii, M. *Dalton Trans.* **2008**, 6709−6723.
(43) Fuchs, Y.; Lofters, S.; Dieter, T.; Shi, W.; Morgan, R.; Strekas, T. C.; Gafney, H. D.; Baker, A. D. *J. Am. Chem. Soc.* **1987**, *109*, 2691−2697.
(44) McFarland, S. A.; Lee, F. S.; Cheng, K. A.; Cozens, F. L.; Schepp, N. P. *J. Am. Chem. Soc.* **2005**, *127*, 7065−7070.
(45) Zigler, D. F.; Wang, J.; Brewer, K. J. *Inorg. Chem.* **2008**, *47*, 11342−11350.
(46) Gennett, T.; Milner, D. F.; Weaver, M. J. *J. Phys. Chem.* **1985**, *89*, 2787−2794.
(47) Caspar, J. V.; Meyer, T. J. *J. Am. Chem. Soc.* **1983**, *105*, 5583−5590.
(48) Kalyanasundaram, K.; Nazeeruddin, M. K. *Inorg. Chem.* **1990**, *29*, 1888−1897.

(49) Ferrari, M. B.; Fava, G. G.; Pelosi, G.; Predieri, G.; Vignali, C.; Denti, G.; Serroni, S. *Inorg. Chim. Acta* **1998**, 275−276.
(50) Zambrana, J. L.; Ferloni, E. X.; Gafney, H. D. *J. Phys. Chem. A* **2009**, *113*, 13457−13468.
(51) Cesar, V.; Bellemin-Laponnaz, S.; Gade, L. H. *Eur. J. Inorg. Chem.* **2004**, 3436−3444.
(52) Fourie, E.; Swarts, J. C.; Lorcy, D.; Bellec, N. *Inorg. Chem.* **2010**, 952−959.
(53) Brewer, K. J.; Murphy, W. R.; Spurlin, S. R.; Petersen, J. D. *Inorg. Chem.* **1986**, *25*, 882−884.
(54) White, T. A.; Arachchige, S. M.; Sedai, B.; Brewer, K. J. *Materials* **2010**, *3*, 4328−4345.
(55) Kober, E. M.; Caspar, J. V.; Lumpkin, R. S.; Meyer, T. J. *J. Phys. Chem.* **1986**, *90*, 3722−3734.
(56) Kalyanasundaram, K.; Gratzel, M.; Nazeeruddin, M. K. *J. Phys. Chem.* **1992**, *96*, 5865−5872.
(57) Unpublished result.
(58) White, T. A.; Knoll, J. D.; Arachchige, S. M.; Brewer, K. J. *Materials* **2012**, *5*, 27−46.